760nm – a new laser diode wavelength for hair removal modules

Martin Wölz*[a], Martin Zorn[a], Agnieszka Pietrzak[a], Alex Kindsvater[b], Jens Meusel[b], Ralf Hülsewede[a], Jürgen Sebastian[a]
[a]JENOPTIK Diode Lab GmbH, Max-Planck-Str. 2, Berlin, Germany
[b]JENOPTIK Laser GmbH, Göschwitzer Str. 29, Jena, Germany

ABSTRACT

A new high-power semiconductor laser diode module, emitting at 760 nm is introduced. This wavelength permits optimum treatment results for fair skin individuals, as demonstrated by the use of Alexandrite lasers in dermatology. Hair removal applications benefit from the industry-standard diode laser design utilizing highly efficient, portable and light-weight construction. We show the performance of a tap-water-cooled encapsulated laser diode stack with a window for use in dermatological hand-pieces. The stack design takes into account the pulse lengths required for selectivity in heating the hair follicle vs. the skin. Super-long pulse durations place the hair removal laser between industry-standard CW and QCW applications. The new 760 nm laser diode bars are 30% fill factor devices with 1.5 mm long resonator cavities. At CW operation, these units provide 40 W of optical power at 43 A with wall-plug-efficiency greater than 50%. The maximum output power before COMD is 90 W. Lifetime measurements starting at 40 W show an optical power loss of 20% after about 3000 h. The hair removal modules are available in 1x3, 1x8 and 2x8 bar configurations.

Keywords: 760 nm, laser diode, quasi-continuous-wave, laser diode stack, hair removal, melanin, transient thermal behavior, reliability

1. INTRODUCTION

Diode laser systems for hair removal have specific requirements that shift the development effort from the semiconductor structure to the packaging. A high optical power density is required from a lightweight handheld device. The cooling effort therefore has to be balanced between these two requirements. On the other hand, the requirements on parameters such as wavelength tolerance or polarization are met by standard devices.

1.1 Laser hair removal

Hair removal is an everyday concern for many people, and since photo-epilation has complemented other, traditional methods, it has therefore become an attractive market for laser manufacturers. The working principle of laser hair removal is to damage the hair structure by heating of the hair shaft and hair follicle. The irradiation in terms of wavelength, pulse duration and intensity is designed to heat the surrounding tissue as little as possible and achieve 'selective photothermolysis.' The skin has an optical window between the light absorption of blood, below 600 nm, and the absorption of water above 1100 nm. Dark hair contains melanin, which absorbs light in this window, with slightly increasing absorption toward the shorter wavelengths.[1] Selectivity can be challenging to achieve when the skin is strongly pigmented or the hair is thin or light compared to the skin. Light is applied for pulse durations between 5 ms and 400 ms, making use of different thermal relaxation times for the hair follicle and epidermis.[2] The light intensity is chosen to minimize treatment time, with the available light sources and the skin cooling concept imposing limits.

Laser diodes have emerged as an important light source emitting around 800 nm. Clinical practice with alexandrite lasers emitting at 755 nm has made this wavelength popular, and it is therefore in demand for robust and lightweight diode laser modules. Clinical studies have not shown a significant difference in treatment efficiency between alexandrite lasers and 800 nm diode laser, possibly because the former have so far been limited to shorter pulse lengths.[3] Typical pulse energies of alexandrite lasers in hair removal have been around 25 J/cm^2. The flexibility of diode lasers emitting around 760 nm allows for a wide parameter choice to establish selectivity in hair removal.

*martin.woelz@jenoptik.com; phone +49-30-677987-100; fax +49-30-677987-199; www.jenoptik.com

Components and Packaging for Laser Systems, edited by Alexei L. Glebov, Paul O. Leisher, Proc. of SPIE
Vol. 9346, 934608 · © 2015 SPIE · CCC code: 0277-786X/15/$18 · doi: 10.1117/12.2077445

1.2 Laser diode assembly

We show in this paper how Jenoptik's patented laser diode stack[4] can be used in hair removal devices. The stack is referred to as 'QCW' stack, an acronym for 'quasi-continuous wave', indicating that the semiconductor laser operation is stationary, while thermal equilibrium is not reached in pulsed operation. In the QCW stack, 3 or 8 laser bars are arranged vertically on an insulating substrate. The 8-bar configuration is shown in Figure 1 (a). This ceramic substrate is passively cooled by mounting on a heat sink with thermally conductive foil. In another configuration, the QCW stack possesses an actively cooled substrate, which includes a cooling water passage. This active QCW stack is offered in a housing. Figure 1 (b) shows a cross section of the active QCW stack on a mount, and Figure 1 (c) depicts the active QCW stack in the housing with 2x8 bar configuration.

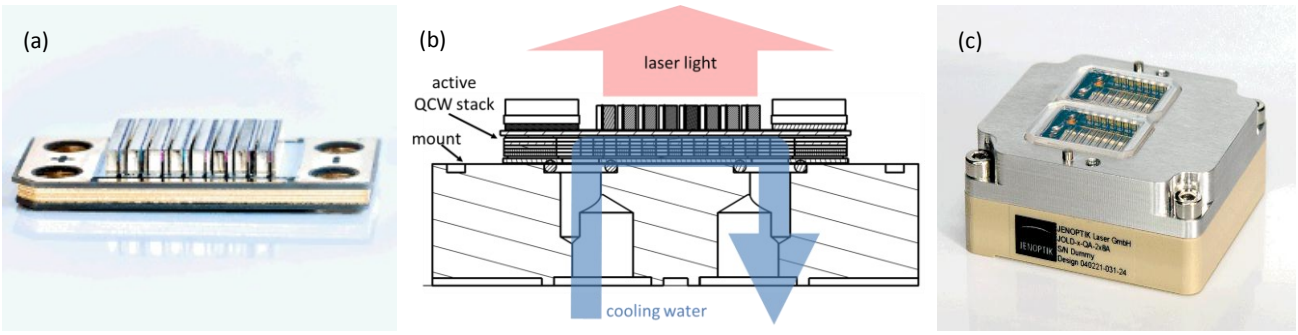

Figure 1. Laser diode packages for QCW application. (a) passively cooled QCW stack, (b) cross section of actively cooled QCW stack on mount with indication of water passage, (c) encapsulated package with active QCW stacks in 2x8 configuration.

The QCW stack housing is designed for a small footprint to keep the cross section of the hair removal handpiece as low as possible. The actively cooled QCW stack is designed for tap water cooling, which greatly facilitates system design in comparison to the de-ionized water requirement of microchannel coolers.

The diode bars in the QCW stack are 10 mm wide and spaced at a pitch of 1.7 mm. The energy intensity of one pulse is $E_p = P_{opt}\, t_p$ / 0.17 cm^2, where P_{opt} is the optical output power per bar and t_p is the pulse length. For a given type of laser bar, the device lifetime is a function of the junction temperature, and hence poses limits on the operating parameters, as we will now discuss in detail.

2. LASER DIODE CW CHARACTERISTICS

The semiconductor laser chip is the heart of the laser module. As a basis for the discussion of the module performance, we present the electro-optical and reliability characteristics of Jenoptik's new 760 nm laser diode bar JDL-BAB-30-19-760-TE-40-1.5.

2.1 Electro-optical characteristics

The laser structure for the 760 nm device was adapted from the proven 808 nm standard structure (see Table 1 in Ref. 5.) The external differential quantum efficiency is η_d = 86.7%. 1 cm-wide laser bars with a resonator length of 1.5 mm are processed with 19 emitters of 150 µm width. The threshold current for this filling factor of 30% is I_{th} = 10.4 A. The laser bar was mounted on a microchannel cooler with the thermal resistance R_{th} = 0.3 K/W and a coolant temperature of 25°C for characterization of the continuous wave (CW) operation. The characteristics of optical output power P_{opt} and wall-plug efficiency vs. current are shown in Figure 2 (a). The pulse spectrum, corresponding to operation at the coolant temperature, is shown in Figure 2 (b) in comparison to the CW spectrum, measured in thermal equilibrium of heat generation and dissipation.

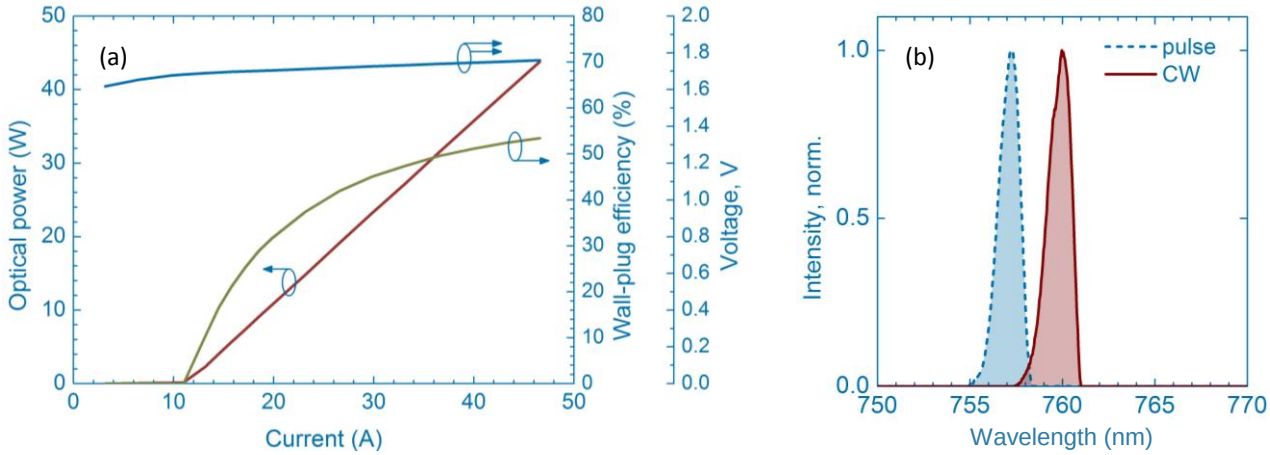

Figure 2. (a) CW power-current and wall-plug efficiency characteristics of a laser bar emitting at 760 nm. (b) spectrum. For cw operation, the laser bar was mounted on a microchannel-cooler with R_{th} = 0.3 K/W at a coolant temperature of 25°C.

In order to predict the behavior of the 760 nm laser under long-pulse operating conditions, where the junction temperature rises significantly above the coolant temperature, the temperature-dependence of the laser parameters I_{th} and η_d can be characterized empirically by exponential relations[6] with T_0 = 126 K and T_1 = 292 K, respectively.

2.2 Reliability

Operating a semiconductor laser with high load leads to degradation. For the design of a laser system, the failure modes have to be known and the operating limits chosen in accord with the requested lifetime. Two significant degradation mechanisms for the 760 nm laser bar are (i) catastrophic optical mirror damage (COMD) and (ii) gradual degradation of the active region.[7] COMD is associated with overheating of the laser facet of the 760 nm device, and occurred at P_{opt} = 90 W per bar. Gradual degradation is typical for GaAs-based laser diodes and is connected in the literature with the creation of point defects. In life testing, this effect manifests itself in decreasing optical output power under continuous operation at constant current. The results from ten devices are shown in Figure 3. Each device is considered to reach end-of-life when the optical power drops to 80% of the initial value.

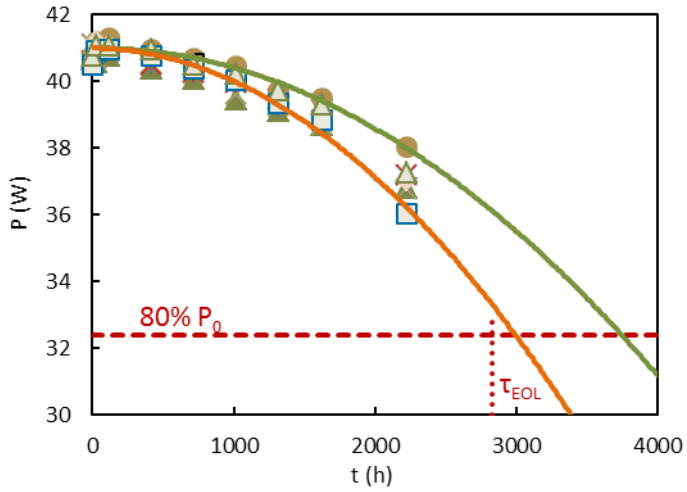

Figure 3. Degradation of the optical output power of 10 test devices in CW operation. Polynomic extrapolations are given for the best and the worst devices under test. Lifetime testing is performed with automatic current control, and end-of-life is the time when the optical power has dropped to 80% of the initial value. The 5% quantile of the end-of-life distribution is indicated as τ_{EOL}. The laser bars were mounted on a microchannel-cooler with R_{th}=0.3 K/W at a coolant temperature of 25°C.

The individual end-of-life times τ_i can be obtained by extrapolation according to ISO 17526. For each device under test, the parameters of a lognormal distribution were calculated.[8] Within a confidence interval of 80%, the lifetime at the 5% quantile of this distribution is 2826 h. This value is marked as τ_{EOL} in Figure 3 and will be considered in the following as the lifetime of the laser diode under CW operation. Gradual degradation is a thermally activated process, and τ_{EOL} follows an Arrhenius behavior with an activation energy E_A reported between 0.6 eV and 1.0 eV.[9]

3. TRANSIENT THERMAL BEHAVIOR

In pulsed operation, as required for laser hair removal, optical power can be extracted from the laser diode in excess of the value obtained during continuous wave operation. The power-limiting factors are COMD and the device degradation at high operating temperature. Therefore, in order to get the most out of a laser diode module, it is essential to understand the thermal behavior in pulsed operation.

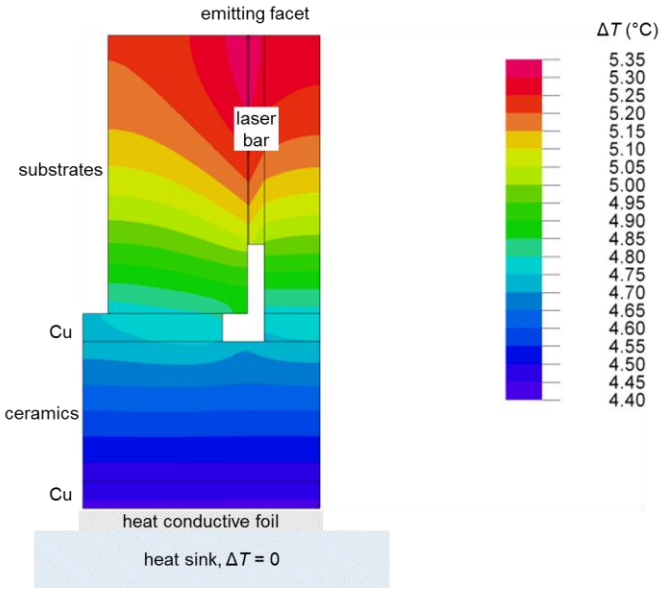

Figure 4. Temperature gradient in the cross-section of one laser bar in the passive QCW stack assembly. The temperatures were calculated for 1 W power dissipation, distributed homogeneously over the laser bar.

First, we analyse the thermal resistance of the individual components of the passively cooled QCW stack. Figure 4 shows the calculated temperature gradient in a section of the passive QCW stack containing one laser bar. The semiconductor is sandwiched between metallic substrates, which are soldered onto the Cu-metallization of the insulating ceramics. The stack is mounted on a heat sink with a foil that can remove 0.01W/mm^2/K of heat, and 1 W of heat is dissipated from the laser bar. The calculation was performed with the *FlexPDE* finite element model (FEM) software. The hottest point is the emitting facet of the laser, running 5.35 K above the heat sink. The biggest contribution to this temperature gradient is the mounting foil, which creates a temperature drop of 4.4 K. In the actively cooled QCW stack, the coolant passes through the ceramics, which can be estimated from the FEM calculation to run about 0.8 K cooler than the laser bar. Table 1 compares the calculated R_{th} for the passive QCW stack, neglecting the temperature distribution inside the laser bar, and the measured R_{th} for the active QCW stack, which is close to the FEM value. The value for the microchannel cooler is given for comparison.

Table 1. Thermal resistance R_{th} of laser diode mountings for 1.5 mm resonator length.

mounting type	passive QCW stack (simulated)	active QCW stack (measured)	microchannel cooler (measured)
R_{th} per laser bar (K/W)	5.34	0.92	0.32

It is evident from Table 1, that even though the active QCW provides much better cooling than the passively cooled stack, diode performance will still be inferior compared to operation on the microchannel cooler. It can be helpful to take into account the local heat capacity in the metallic substrates holding the laser bar. The substrates absorb heat at turn-on and delay the thermal equilibrium. To quantify, how much heat a semiconductor package can dissipate in pulsed operation, the transient thermal resistance is commonly used, as discussed in the following.

3.1 Pulsed operation of the passive QCW stack

Laser diodes as a heat source can be characterized by their thermal response to changes in power dissipation $P(t)$. From the unit power step response, the Z_{th} function, arbitrary pulse and temperature patterns can be calculated.[10] The curve in Figure 5 (a) shows the thermal behavior at turn-on: initially, the heat capacity adjacent to the laser bar absorbs the heat, and the temperature difference $\Delta T(t) = P(t)Z_{th}(t)$ between the junction and the heat sink remains low. At about t = 3s, CW operation is attained, and the Z_{th} function assumes the value of the thermal resistance R_{th} = 5.34 K/W. The function was calculated with *FlexPDE*. For reference, the curve can be approximated as a Foster RC Network, i.e. by

$$Z_{th}(t) = \sum_{i=1}^{n} r_i (1 - e^{-t/\tau_i}) \tag{1}$$

with the contributions to the thermal resistance r_i and their characteristic times τ_i given in the inset of Figure 5 (a).

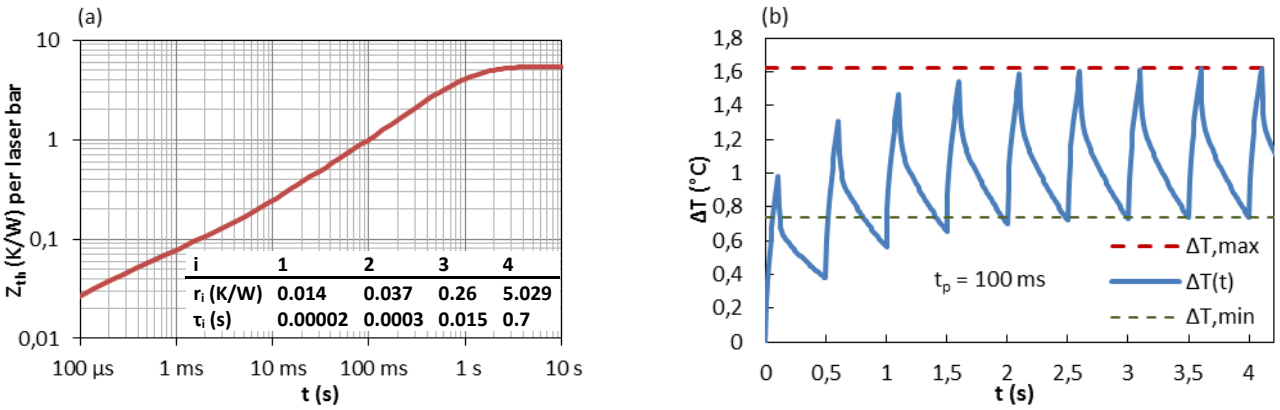

Figure 5. Transient thermal behavior of the passively cooled QCW stack. The stack is mounted on a heatsink with conductive foil, allowing a heat transfer of 0.01W/mm^2/K. (a) Thermal impedance Z_{th} of one laser bar. The CW operating temperature is attained after 3s. Fit parameters are given in the inset. (b) Temperature pattern under pulsed operation with t_p = 100 ms, *d.c.* = 20%. Power dissipation during turn-on is 1 W per bar.

Hair removal applications differ significantly from classic applications of QCW diode lasers. Whereas in solid-state-laser pumping pulse lengths are around $t_p \approx 1$ ms, and the Z_{th} is then almost two orders of mangnitude below R_{th}, leading to negligible heating, hair removal requires $t_p \approx 100$ ms. One reads from Figure 5 (a) that a fifth of the CW temperature rise is already achieved in one pulse. Matters worsen in repetitive operation where the laser is not allowed to cool completely before the next pulse. Figure 5 (b) shows the calculated temperature pattern for pulsed operation with pulse length t_p = 100 ms and 20% duty cycle. At about t = 3s, the average temperature has settled, and ΔT oscillates between ΔT_{max} and ΔT_{min}. The curve for $\Delta T(t)$ was obtained by summing up for any point in time the thermal responses to all previous pulses,[11] i.e. evaluating the convolution integral

$$\Delta T(t) = \int_0^t Z_{th}(t-\tau) P(\tau) d\tau \,. \tag{2}$$

The comparatively long pulse lengths in hair removal call for a low value of R_{th} and necessitate integration of the actively cooled QCW stack into the handpiece. Now that we introduced the concept of the transient thermal behavior in the laser diode package, we turn to operating the actively cooled QCW stack, where we make use of measured values for the pulsed operation.

3.2 Diode performance in the active QCW stack under ultra-long pulse operation

The optical output power suffers from thermal roll-over if the laser diode runs hot. This effect is shown in Figure 6 for different ultra-long pulse operating conditions. 760 nm laser bars with 30% fill factor were mounted on an active QCW stack with coolant at 25°C, and the optical output was integrated with a thermal sensor over different pulse lengths. The optical output power P_{opt} is given per bar, and is seen to be almost linear with current up to 80 A for pulse length t_p = 50 ms, but only up to about 30 A for t_p = 100 ms. Aside from the low output power, operating close to thermal roll-over leads to high junction temperatures that are detrimental to the laser lifetime.

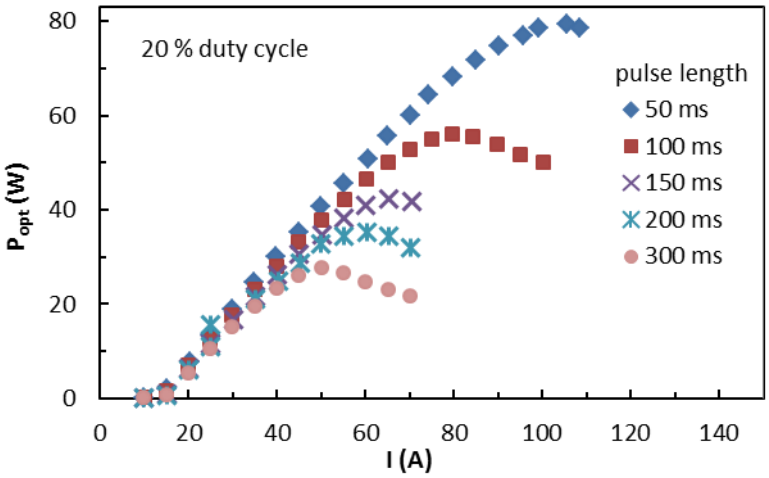

Figure 6. Average optical pulse power per bar for different pulse lengths at 20% duty cycle. The optical power is integrated over the pulse length with a thermal sensor. 760 nm laser bars with 30% fill actor were mounted in an active QCW stack. Heating of the laser leads to thermal roll-over, which becomes more pronounced for longer pulse lengths.

We now estimate the temperature rise during ultra-long pulse operation experimentally. We use the wavelength shift $\Delta\lambda/\Delta T$ = 0.23 nm/K to measure the temperature. Figure 7 shows the reference spectrum acquired in very short pulses (dashed line), representing ΔT = 0, and spectra from long-pulse (t_p = 100 ms, *d.c.* = 45%) and CW operation. CW operation establishes thermal equilibrium, and the spectral width is therefore similar to the reference. The long-pulse spectrum appears broad, because the device temperature changes during the measurement.

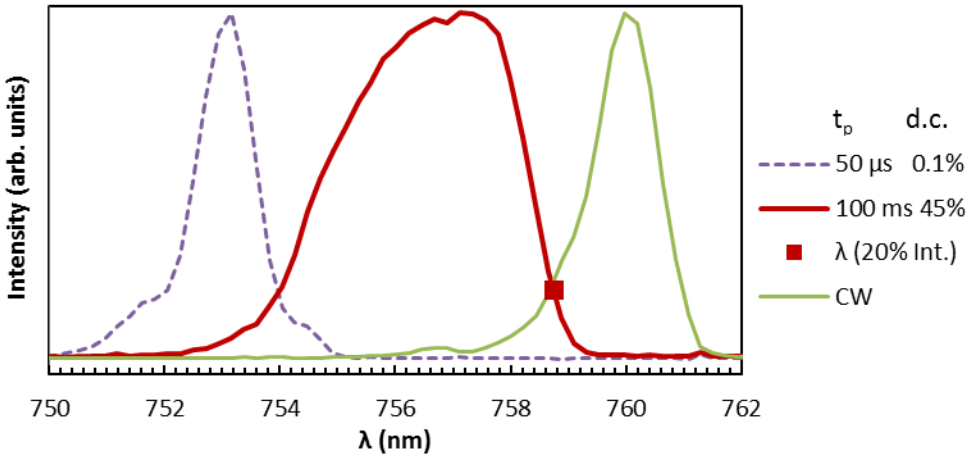

Figure 7. Spectra for short-pulse, long-pulse and CW operation. The 760 nm laser diode was subjected to a test current of 23 A in the actively cooled QCW stack.

The maximum temperature reached during long-pulse operation can be estimated by the long-wavelength component $\lambda_{20\%}$ of the spectrum, taken at 20% of the peak intensity (indicated by the square). This procedure for determination of ΔT was applied to a series of pulse spectra measurements, and the corresponding wall-plug efficiencies were also measured. The resulting values $\Delta T / P$ can be interpreted as data points for Z_{th}-functions, as shown in Figure 8. It is evident that large duty cycles prevent cooling of the laser diode during the turn-off times, and hence the minimum Z_{th} rises with the duty cycle. This experimental set of curves for the active QCW stack can be used to estimate the junction temperature during the pulse for arbitrary pulse parameters, analogously to the calculated curve for the passive QCW stack in Figure 5 (a).

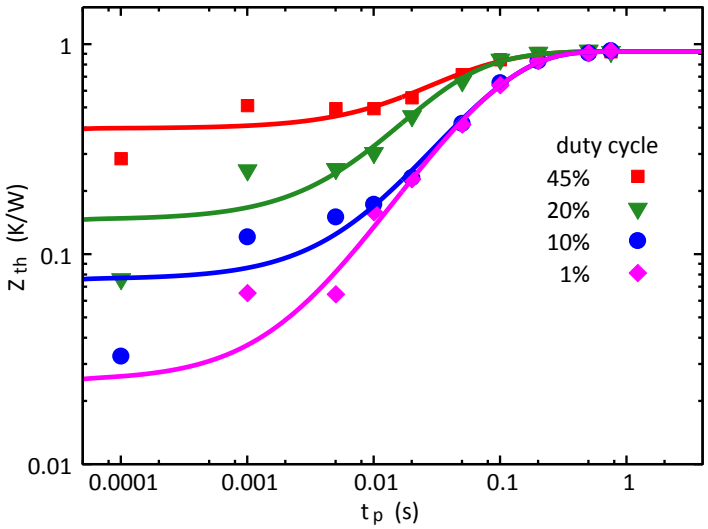

Figure 8. Transient thermal impedance curves for QCW stack with active cooling. The measured values represent the temperature rise during a pulse of length t_p. The temperature was deduced from the redshift of the long-wavelength component $\lambda_{20\%}$ in the pulse spectra.

Strictly speaking, our experimental approach to the pulse spectra only gives an estimate for the maximum junction temperature during the pulse, and does not allow us to obtain a full picture as in Figure 5 (b). For our purpose of studying the maximum useful output power, however, this method is helpful. The Foster model parameters r_i and τ_i for approximate Z_{th}-curves are given for reference in Table 2, and are valid for t_p from about 1 ms.

Table 2. Model parameters for transient thermal impedance curves of one laser bar in the QCW stack with active cooling. The parameters are valid for t_p from about 1 ms for different duty cycles (d.c.), as shown in Figure 8. R_{th} in CW operation is 0.922 K/W per laser bar.

	i	1	2	3
	τ_i (s)	0.00001	0.03	0.1
r_i (K/W)	1% d.c.	0.025	0.128	0.769
	10% d.c.	0.076	0.069	0.777
	20% d.c.	0.146	0.567	0.209
	45% d.c.	0.397	0.299	0.226

3.3 Reliability considerations under ultra-long pulse operation

We now use the above information collected so far and determine which pulse parameters are permissible for reliable operation of the actively cooled QCW stack. With the thermal impedance $Z_{th}(t)$ obtained from experiments in Figure 8 and the laser parameters given in section 2, the junction temperature during the pulse can be calculated. The result is shown in Figure 9 (a), where the curves connect pulse parameter sets leading to equal junction temperature. Mirror facet degradation observed as COMD poses an upper limit on the useful pulse power which is shown by the dashed lines in Figure 9. For operation below the COMD level, the lifetime depends on the temperature reached during the pulse.

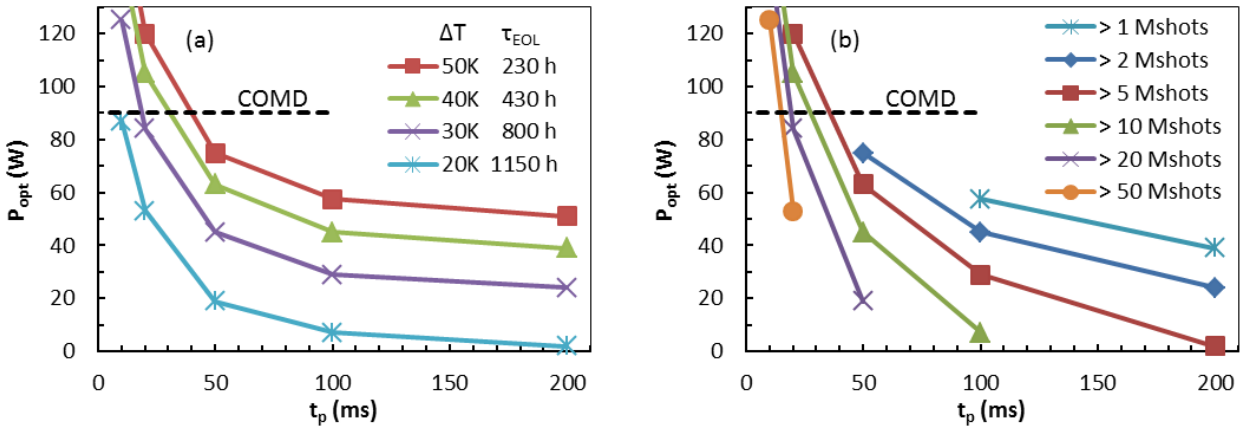

Figure 9. COMD limit and thermal limit to optical pulse power at 20% duty cycle. (a) The curves connect pulse parameters t_p, P_{opt} with equal maximum device temperature and, hence, equal device lifetime under CW operation. The temperature dependence of the lifetime is given for $E_A = 0.6$ eV. (b) The curves denote the numbers of turn-on cycles that add up to the expected CW lifetime.

From section 2.2 we know the lifetime τ_{EOL} = 2826 h at ΔT = 11.5 K in CW operation. For the present discussion we assume an Arrhenius behavior of the lifetime with $E_A = 0.6$ eV.[12] The corresponding CW lifetimes are noted in the key to Figure 9 (a). A temperature increase of 10 K reduces the lifetime roughly to one half. Gradual degradation occurs only during the on-time in pulsed operation. For the operating parameters under consideration so far, Figure 9 (b) gives the number of achievable pulses in millions of cycles (Mshots). If a lifetime of 5 Mshots is desired for operating at t_p = 100 ms, *d.c.* = 20%, for example, P_{opt} must be limited to 30 W. It is important to note that the achievable optical power is much lower in this case than in CW operation on a microchannel heatsink as shown in Figure 2 (a), even though greater lifetime is achieved there. The reason is, of course, the long pulse length and the much larger R_{th} of the actively cooled QCW stack compared to the microchannel cooler. Our analysis also provides, however, quantitative information on the increased lifetime for shorter pulse lengths.

A more careful analysis of the lifetime under pulsed operation would require a number of refinements. One should (i) undertake an experimental confirmation of E_A, and (ii) deliver an experimental proof that the cumulated gradual degradation in pulsed operation equals the power loss in CW operation.

4. CONCLUSION

Diode laser modules are readily integrated into hair removal handpieces. We have shown how to determine useful operating parameters as a function of the required lifetime. In consequence, the greatest benefit from the laser device can be obtained, if the load cycles in clinical use can be specified. Our analysis can be easily extended to calculating the cumulative ageing effect of mixed operating regimes, each leading to degradation at different rates. With the numerous approximations, the lifetime estimations given here are not a replacement for a test, but can be used to define the life test parameters which are most meaningful to the application.

ACKNOWLEDGMENTS

The Z_{th} function for the passively cooled QCW stack was calculated by Dirk Lorenzen. The authors are grateful to Dirk Schweitzer for his help with the pulsed temperature profile.

REFERENCES

[1] Lask, G., Eckhouse, S., Slatkine, M., Waldman, A., Kreindel, M. and Gottfried, V., "The role of laser and intense light sources in photo-epilation: a comparative evaluation," J. Cosmet. Laser Ther. 1, 3-13 (1999).

[2] Lepselter, J. and Elman, M., "Biological and clinical aspects in laser hair removal," J. Dermatol. Treat. 15, 72-83 (2004).

[3] Gottschaller, C. and Hohenleutner, U., "Laser- und Lichtepilation," in Landthaler, M. and Hohenleutner, U. (Eds.), [Lasertherapie in der Dermatologie], Springer Medizin Verlag, Heidelberg, 179-192 (2006).

[4] EP patent no. 1977486.

[5] Zorn, M., Hülsewede, R., Pietrzak, A., Meusel, J., Wölz, M. and Sebastian, J., "Reliable single emitters and laser bars for efficient CW-operation in the near-infrared emission range," Proc. SPIE, 9348-20 (2015).

[6] Erbert, G., Bärwolff, A., Sebastian, J. and Tomm, J., "High-Power Broad-Area Diode Lasers and Laser Bars," in Diel, R. (Ed.), [High-Power Diode Lasers], Springer, Berlin & Heidelberg, 173-223 (2000).

[7] Jiménez, J., "Laser diode reliability: crystal defects and degradation modes," C. R. Phys. 4, 663-673 (2003).

[8] Lorenzen, D., Meusel, J., Schröder, D. and Hennig, P., "Passively cooled diode lasers in the cw power range of 120 to 200W," Proc. SPIE, 68760Q (2008).

[9] Waters, R., "Diode laser degradation mechanisms: A review," Prog. Quantum Electron. 15, 153-174 (1991).

[10] Schweitzer, D., "Thermal Transient Multisource Simulation Using Cubic Spline Interpolation of Zth-Functions," Proc. 12th THERMINIC, Nice, France, 123-127 (2006).

[11] "Using Power MOSFET Z_{th} Curves," NXP Application Note 11156 (2012).

[12] Ueda, O., [Reliability and degradation of III - V optical devices], Artech House, Boston, (1996).